Taylor & Francis
Taylor & Francis Group

Fullerenes, Nanotubes and Carbon Nanostructures

ISSN: 1536-383X (Print) 1536-4046 (Online) Journal homepage: http://www.tandfonline.com/loi/lfnn20

# Morphology and surface structure of nanocarbon allotropes: a comparative study

M. Hernandez-Ortiz, Y. Estevez-Martinez, S. M. Duron, I.L. Escalante-Garcia, M. Vega-Gonzalez & V. M. Castano

**To cite this article:** M. Hernandez-Ortiz, Y. Estevez-Martinez, S. M. Duron, I.L. Escalante-Garcia, M. Vega-Gonzalez & V. M. Castano (2016): Morphology and surface structure of nanocarbon allotropes: a comparative study, Fullerenes, Nanotubes and Carbon Nanostructures, DOI: 10.1080/1536383X.2016.1146706

**To link to this article:** http://dx.doi.org/10.1080/1536383X.2016.1146706

Accepted author version posted online: 06 Feb 2016.

# Morphology and surface structure of nanocarbon allotropes:

# a comparative study

M. Hernandez-Ortiz[a], Y. Estevez-Martínez[a,b], S. M. Durón[a], I.L. Escalante-García[a], M. Vega-González[c], V. M. Castaño[d]

[a]Facultad de Ciencias Químicas Campus Siglo XXI, Universidad Autónoma de Zacatecas, Edificio 6 Km 6 Carretera Zacatecas-Guadalajara, Ejido la Escondida, Zacatecas, Zac., Mexico 98160. [b]Nano Coating Technologies SA de CV, Paseo de las Palmas 555, Miguel Hidalgo, Distrito Federal, México, 11000, [c]Centro de Geociencias Campus Juriquilla, Universidad Nacional Autónoma de México, Boulevard Juriquilla 3001, Querétaro, Qro., México 76230, [d]Departamento de Ingeniería Molecular de Materiales del Centro de Física Aplicada y Tecnología Avanzada Campus Juriquilla, Universidad Nacional Autónoma de México, Boulevard Juriquilla No. 3001, Querétaro, Qro., México 76230.



## ABSTRACT

Different carbon allotropes, including Vulcan Carbon (VC), MultiWall carbon nanotubes (MW), Graphene (Graph) and nanoDiamonds (nD) were processed by chemical purification and treated in a mixture of $H_2SO_4$-$HNO_3$. The materials were characterized by

 

Infrared (IR) and Raman spectroscopy, as well as by scanning (SEM) and transmission (TEM) electron microscopy. Oxidative differences are indicated by Raman through the G band (~1570 $cm^{-1}$), D band (~1340 $cm^{-1}$) and G' band (~2684 $cm^{-1}$). The crystal size (La) and purity, relative to the amorphous carbonaceous material, were studied as well, along with the morphological changes induced by the treatments.



 

## INTRODUCTION

The different allotropes of carbon are the focus of great attention nowadays, including their synthesis, characterization and application of a variety of carbon-based nanostructured materials, according to the spatial orientation of the hybridized orbitals, such as graphene, carbon

nanotubes, nanodiamonds, and mesoporous carbon, all showing unique and novel properties [1]. Oxidation is frequently used for purification of carbon-like materials, since, when properly functionalized, these material open new venues for novel materials design [2]–[4]. Specifically, purification has been extensively explored to achieve certain insertion of defects and/or breakdown of the original carbon structure, to attach some functional groups [2], [5]–

 

[8]. Therefore, functionalized carbons are of great relevance, for example, for applications such as chemical and gas sensors [9], [10].

Vulcan carbon (VC), also known as carbon black, is practically an ideal support because of its high surface area, good electric conductivity and high porosity. VC consists of agglomerated spherical primary particles, comprising graphitic and amorphous-like portions, with average particle sizes between 10 and 100 nm, depending on the specific mechanism of formation [11]–[13]. Opposite to VC, nanodiamond (nD) has superior properties, such as electrical insulation, high thermal conductivity, chemical inertness, optical transparency (from UV to IR), high mechanical stability and corrosion resistance, and have triggered active research activities on device-oriented applications, and it is, nowadays, used in electronic industry as field emitter [14]–[18].

As for the carbon nanotubes (CNTs), their mechanical, thermal and electrical properties are outstanding. Therefore, a large number of experimental and theoretical studies have been dedicated to their chemical and structural characterization [2], [19], [20]. Since their electrical and mechanical conductivity decrease when increasing the number of defects, thus their graphitic degree of orientation on the external walls of the multi-wall carbon nanotube (MW) reduces. The thermal properties of the CNTs are more similar to a graphitic plane in less ordered forms of carbon, being able to stand over 1000 °C [21]–[23]. As compared to CNTs, Graphene (Graph) is less expensive to produce and more miscible, due to its large surface area. Studies have reported hardness, electrical conductivity and thermal properties of functionalized Graph. Furthermore, organosilane-functionalized Graph has shown a high thermal degradation and high tensile strength [24].

Raman spectroscopy is known to be quite sensitive to a wide range of disordered carbon allotropes, such as low-dimensional crystals or small grain sized polycrystalline materials. However, the detailed interpretation of the Raman spectra of carbonaceous materials has generated considerable debate among the experts.

in the literature, due to the complex microstructure of these systems [25], Raman spectroscopy was first used to characterize different carbon species not long after the discovery of the Raman Effect in 1928 [26], prior to the knowledge of the very existence of carbon nanostructures [2]. We now know that carbon is a unique element that can give rise to materials as diverse as diamond, graphite, fullerenes, carbon nanotubes, and nanostructured disordered and amorphous carbons [27]. The full understanding of Raman spectra of carbon nanomaterials led to the extension of this technique from simple carbon allotrope detection (fingerprinting) to analysis of the dimensions and ordering [18], [28].

Accordingly, the purpose of this present work is to analyze the most relevant structural information on carbonaceous nanomaterials, both functionalized and unfunctionalized, aiming to understand the significant differences of the chemical oxidative purification by Raman spectroscopy and other complementary techniques. The unfunctionalized nanocarbon allotropes included VC, nanodiamonds nD, MW and Graph, and their functionalized nanocarbons (VC-f, nD-f, MW-f and Graph-f).

## MATERIALS AND METHODS

### Materials and reagents

VC, XC-72 carbon black was purchased from Sigma–Aldrich Co., USA. nD powder was supplied from Saint Gobain New Materials Development Co., USA. Graphene was prepared from natural sources by an improved Hummer's method [29]. MW were obtained from Sun Nanotech Co. Ltd, which produced them by chemical vapor deposition, with a diameter from 10 to 30 nm and lengths 1 to 10 μm, with a purity >90% and surface area of 90 to 350$m^2g^{-1}$. Nitric acid ($HNO_3$, purity > 70%) and sulfuric acid ($H_2SO_4$, purity > 95-99%) were purchased from Sigma-Aldrich Co. Ltd.

### Functionalization

Based on a previous report [30], the purification/oxidation of all materials used in this work (except graphene) was achieved in liquid phase with a 3:1 mix of $NHO_3$:$H_2SO_4$ at 80 ˚C for 3 h in a reflux process. The resulting material was vacuum-washed to a neutral pH with deionized water. Graphene oxide was prepared according to a previous report from our group [29].

## Characterization techniques

Samples were observed in a HITACHI TM1000 scanning electron microscope (SEM) at 15 KV with a backscattered detector, after dispersed in ethanol. Samples, as pellets of KBr, were analyzed in a Bruker Tensor 27 infrared (IR) spectrometer. The resolution was of 4 $cm^{-1}$ at 32 scans between 4000 and 400 $cm^{-1}$. Raman spectra were recorded at room temperature using a

Renishaw Raman system, model 1000, with a 200-mW argon-ion laser, at an excitation wavelength of 514.5 nm and an integration time of 30 s, except for nD, which was characterized by a Senterra Bruker Raman scattering instrument with a 785 nm laser. Transmission electron microscopy (TEM) of the carbons was performed in a JEOL JEM-1010 instrument.



## RESULTS AND DISCUSSION

Raman characteristic bands for the carbon nanostructures with hibridation $sp^2$ and $sp^3$, such as CNTs [31], Graph [32], VC [25] and nD [33], appear at ~1570 $cm^{-1}$ (G band), ~1340 $cm^{-1}$ (D band) and ~2684 $cm^{-1}$ (G' band) [19], [34]. To verify the oxidation/purification of the nanostructures, some publications [35], [36] consider the G band as an indicator of purity and crystallinity. On the other hand, some papers [37], [38] evaluate the purity of these carbon allotropes by the D band, characteristic of the diamonds, because it is sensitive to the carbonaceous impurities and structural defects in the graphitic sp2 networks, different to the G band. The intensity of the G' band, according to other authors [31], [32], is proportional to the purity of the MW and Graph, due to the absence of nano-carbons and it provides unambiguous information about the number of constituents in the Graph layers. Hence, in this work, we related the areas of the G'/G, G'/D and D/G bands to establish a relationship of the purity of nanocarbon materials in the Graph and MW with regard to VC. The dimensionless area values of G, D and G' bands and its relations, could thus indicate the carbonaceous purification of these nanomaterials. Also, in addition to the intensity of the band, its width is very relevant, according

to full-width-at-half-maximum (FWHM) widely-reported parameter [37]. For example, the D band is broader in graphite than in other nanocarbons, with 29 and 25 $cm^{-1}$ for CNTs.

On the other hand, the lateral average size of graphitic crystallites by $L_a$ [39] was evaluated by using the empirical formula:

$$L_a = 4.35 \frac{I_G}{I_D} \, [nm] \qquad (1)$$

Where $I_G$ and $I_D$ correspond to the intensity of the G and D bands, respectively.

According to Figure 1a and Figure 1b, the characteristic Raman spectra for Graph, MW, VC and nD, are present [25], [33], [37]. To confirm the oxidative activity of the acids over these carbon allotropes, we present calculations of $L_a$ for the intensities and the R2 = D/(D+G+D'), G'/G, G'/D and D/G bands area values for each carbon, both untreated and purified. No significant difference for the oxidized carbons was observed. These samples show high microcrystalline planar size, i.e. $L_a$, higher than 4 nm; high order $sp^2$ bonded carbons [25]. VC shows a significant higher degree of structural order arising from larger graphitic domains ($L_a$ = 21–22 nm), as compared to all other carbons, which show low $L_a$ values in the range of 4 to 6 nm. Moreover, only VC shows a marked difference of intensity in the bands G and D, which is a hint for higher structural order [13], [40]. VC has high crystallinity due to high $L_a$ and R2 (D/D+G+D'), and does not contain amorphous carbonaceous material for high values of G'/D and G'/G, and with a low value in D/G. This result is similar for perfect graphene with two or

three layers [32], with the difference that the crystal size $L_a$ is larger than in the nanostructured materials, as calculated and reported in this work. Accordingly, the oxidation/purification for every carbon material is clear, as revealed by the increase of $L_a$ and R2 and to the amorphous carbons removal for increase in G'/D and G'/G, and the low value in D/G for VC, MW and Graph. For nD, the D band intensity decreased because their oxidation is done through the generation of structural defects in its $sp^3$ hybridization [41]. Figure 1c, confirms the relationship between FWHM and the area value for all the Raman bands.

IR spectra for the functionalized and unfunctionalized carbons are shown in Figure 2, VC and VC-f (a) have few similar features: VC-f spectrum presents some noise that overshadows some characteristic peaks, but the bands at 3500 - 3900 $cm^{-1}$, corresponding to O–H groups, C=O (carboxylic acid) and C=C in aromatic ring groups at 1750 - 1550 $cm^{-1}$ in different environments, are clearly seen. Also, C–$H_x$ stretching vibrations $sp^3$ where x=3 (symmetric) and x=2 (asymmetric) are present at 2850 and 2925 $cm^{-1}$ bands. These peaks appear weak in the IR spectrum of VC. However, the others bands described are not visible and a well-defined peak related to C=O stretching vibration at 1250 $cm^{-1}$ band appears [30], [42]. For MW (b), the wide stretching vibrations for O−H peak centered at 3850 $cm^{-1}$ are displaced to 3630 $cm^{-1}$ for MW-f. The complex bands around 1540, 1050 and 665 $cm^{-1}$ in the MW spectrum are attributed to C=C stretching for carboxylate salts, C−O−C stretching and C–H vibration of vinyl alkene, respectively [43], [44]. These bands are defined for MW-f but displaced to 1240 and 780 $cm^{-1}$ that would involve C–O and C–H stretching vibrations for aromatic benzene, respectively. A broad band of O–H stretching at 3000-3450 $cm^{-1}$ and a peak of the C–H stretching at 2950 $cm^{-1}$

appear only for functionalized MW [9]. The IR spectrum for nD and nD-f (c) at 2800-3600 $cm^{-1}$ clearly show the C–H and O–H stretching of the carboxylic acid on its surfaces, with a shoulder assigned to C–H stretching vibrations around 2940 $cm^{-1}$ on the C(100) plane [45], [46]. Most defined differences between nD and nD-f IR spectra, are the C-H, C-O or C=C stretch vibrations in a broad absorption at 1100 $cm^{-1}$ [42]. The other peak at 1380 $cm^{-1}$ is more clear in nD and it corresponds to C-H vibrations, that are more intense when next to a C–O group [30]. Clear differences are present in the IR spectra of Graph and Graph-f (d), mainly the broad band in the 2800-3650 $cm^{-1}$ region, due to the carboxylic O-H stretches and peaks of the C-H stretching are present only in Graph-f. Also, this material exhibits well-defined bands corresponding to Graph at 1720, 1580 and 1380 $cm^{-1}$; the first two are assigned to C=O stretching for a six member carbon ring structure and for carboxylate salts, respectively; and the last peak to C−OH stretching [44]. Moreover, C-O groups present in the bands at 1100, 1180 and 1250 $cm^{-1}$ correspond to alcohols and carboxylic acids.

Molecular vibrations may be detected and measured either by an infrared spectrum or indirectly from a Raman Spectrum. This means that the two types of spectra are complementary to each other if a full characterization of carbon allotropes is to be achieved. Infrared is the most informative for organic chemists because most functional groups are not centrosymmetric [47]. Raman provides information relevant for the chemical analysis of nanocarbon allotropes.

Figure 3 shows the surface morphology of the nanocarbon allotropes studied in this work. 2D Graph is the basic building block for graphitic materials of other dimensionalities (0D fullerenes, 1D nanotubes and 3D graphite). Functionalized Graph was produced through reduction of Graph oxide and displays multiple-layer flexible sheets, different from the typical wrinkled and folded morphology of the Graph sheets (a and b). The surface morphologies of nD and nD-f (c and d, respectively) do not show significant changes. Both samples display clusters of carbon spheres, but nD-f presents higher resolution. It can be seen that the two consist of a heterogeneous agglomeration of micrometer-sized spherical secondary particles. The size of these secondary particles is estimated by considering them as spherical particles smaller than the relatively large particles called agglomerates or tertiary structures [48]. Likewise, morphology VC and VC-f exhibits a structurally heterogeneous single-layer planes structure [13], [49] (e and f); this is confirmed by the TEM images, Figure 4. The impurities have been removed and the clustering of MW is significantly improved (h). MW-f is a disordered entanglement, because of the impurities present. In all carbon morphologies, the presence of lighter elements, commonly grouped in organic particles [50], clearly displayed in oxidized carbons, was detected.

To support the Raman spectroscopy, TEM observation was conducted ,as shown in Figure 4. nD and nD-f particles are well-defined with a diameter ranging between 5 to 9 nm, as shown in the TEM micrographs (c and d). In both samples, all primary particles are nearly spherical-shaped and clustered in larger aggregates. Therefore, nD and nD-f do not present

significant difference. In addition, the surface of the VC samples shows carbon layers. VC presents rough surface layers, while that of VC-f is a smooth layer (a and b). After oxidation, the VC-f layers are well ordered, since functional groups generate stacks of planar layers, as a kind of exfoliation on the outer sheets of VC. The TEM micrograph for MW-f shows ~15 nmnanotubes, slightly narrower than that of the original MW (e and f). MW-OH clearly shows the expected defects on the walls of the nanotubes, as it has already been reported by using high resolution TEM [51]. The typical morphology of Graph and Graph-f is shown in TEM images already reported [29, 51].



## CONCLUSIONS

We have reported the comparative characterization, by using spectroscopies and microscopies, of different nanocarbon allotropes, including raw (VC, nD, MW, Graph) and treated (VC-f, nD-f, MW-f, Graph-f). The results indicate that there is a relative increase in the various hydroxyl, carbonyl and carboxyl carbon groups of the acid-treated, as seen by IR. On the other hand,

according to the values of $L_a$ and the different Raman studie,s VC and VC-f have highly oriented pyrolytic graphite (HOPG) and their size is within the nano scale.



**Acknowledgements**

 

The authors are grateful to Mrs. Alejandra Núñez Pineda, Mrs. Lourdes Palma-Tirado and Dr. Genoveva Hernández-Padron of Universidad Nacional Autonoma de Mexico; Dr. Sergio Jiménez-Sandoval and Mr. Francisco Rodríguez Melgarejo of CINVESTAV-Qro. for their technical support. We would like to thank Edgar Jimenez-Cervantes Amieva for his aid with the Graph and Graph-OH samples preparation. M. Hernández-Ortiz is a recipient of post-doctoral fellowship from CONACyT and of "For Woman in Science L'Oreal-UNESCO-CONACyT-AMC 2015" fellowship.



 

 

 

## REFERENCES

[1] V. E. Borisenko and S. Ossicini, *What is what in the Nanoworld: A Handbook on Nanoscience and Nanotechnology*. John Wiley & Sons, 2013.

[2] K. Tanaka and S. Iijima, *Carbon nanotubes and graphene*. Newnes, 2014.

[3] C. S. Kumar, *Raman spectroscopy for nanomaterials characterization*. Springer Science & Business Media, 2012.

[4] V. Datsyuk, M. Kalyva, K. Papagelis, J. Parthenios, D. Tasis, A. Siokou, I. Kallitsis, and C. Galiotis, "Chemical oxidation of multiwalled carbon nanotubes," *Carbon*, vol. 46, no. 6, pp. 833–840, May 2008.

[5] K. Awasthi, R. Kumar, H. Raghubanshi, S. Awasthi, R. Pandey, D. Singh, T. P. Yadav, and O. N. Srivastava, "Synthesis of nano-carbon (nanotubes, nanofibres, graphene) materials," *Bull. Mater. Sci.*, vol. 34, no. 4, pp. 607–614, 2011.

[6] M. Monthioux, *Carbon meta-nanotubes: Synthesis, properties and applications*. John Wiley & Sons, 2011.

[7] G. A. Olah, G. S. Prakash, J. Sommer, and A. Molnar, *Superacid chemistry*. John Wiley & Sons, 2009.

[8] A. Radoi, D. Compagnone, M. A. Valcarcel, P. Placidi, S. Materazzi, D. Moscone, and G. Palleschi, "Detection of NADH via electrocatalytic oxidation at single-walled carbon



 

nanotubes modified with Variamine blue," *Electrochimica Acta*, vol. 53, no. 5, pp. 2161–2169, 2008.

[9] H. Peng, L. B. Alemany, J. L. Margrave, and V. N. Khabashesku, "Sidewall carboxylic acid functionalization of single-walled carbon nanotubes," *J. Am. Chem. Soc.*, vol. 125, no. 49, pp. 15174–15182, 2003.

[10] S. Hussain, S. S. Islam, and T. Islam, "Purification and Oxidation Studies of Multiwall Carbon Nanotubes using Raman Spectroscopy," *Asian J. Chem.*, vol. 23, no. 12, p. 5639, 2011.

[11] A. Zana, J. Speder, N. E. Reeler, T. Vosch, and M. Arenz, "Investigating the corrosion of high surface area carbons during start/stop fuel cell conditions: A Raman study," *Electrochimica Acta*, vol. 114, pp. 455–461, 2013.

[12] L. Bokobza, J.-L. Bruneel, and M. Couzi, "Raman spectroscopic investigation of carbon-based materials and their composites. Comparison between carbon nanotubes and carbon black," *Chem. Phys. Lett.*, vol. 590, pp. 153–159, 2013.

[13] M. Pawlyta, J.-N. Rouzaud, and S. Duber, "Raman microspectroscopy characterization of carbon blacks: Spectral analysis and structural information," *Carbon*, vol. 84, pp. 479–490, 2015.

[14] S. Szunerits and R. Boukherroub, "Different strategies for functionalization of diamond surfaces," *J. Solid State Electrochem.*, vol. 12, no. 10, pp. 1205–1218, 2008.

[15] T. Tsubota, S. Tanii, S. Ida, M. Nagata, and Y. Matsumoto, "Chemical modification of diamond surface with various carboxylic acids by radical reaction in liquid phase," *Diam. Relat. Mater.*, vol. 13, no. 4, pp. 1093–1097, 2004.

[16] M. Mermoux, A. Crisci, T. Petit, H. A. Girard, and J.-C. Arnault, "Surface Modifications of Detonation Nanodiamonds Probed by Multiwavelength Raman Spectroscopy," *J. Phys. Chem. C*, vol. 118, no. 40, pp. 23415–23425, 2014.

[17] A. V. Shushkanova, L. Dubrovinsky, N. Dubrovinskaya, Y. A. Litvin, and V. S. Urusov, "Synthesis and in-situ raman spectroscopy of nanodiamonds," in *Doklady Physics*, 2008, vol. 53, pp. 1–4.

[18] V. Mochalin, S. Osswald, and Y. Gogotsi, "Contribution of functional groups to the Raman spectrum of nanodiamond powders," *Chem. Mater.*, vol. 21, no. 2, pp. 273–279, 2008.

[19] J. H. Lehman, M. Terrones, E. Mansfield, K. E. Hurst, and V. Meunier, "Evaluating the characteristics of multiwall carbon nanotubes," *Carbon*, vol. 49, no. 8, pp. 2581–2602, Jul. 2011.

[20] A. L. Martínez-Hernández, C. Velasco-Santos, V. Castano "Carbon nanotubes composites: processing, grafting and mechanical and thermal properties," *Curr. Nanosci.*, vol. 6, no. 1, pp. 12–39, 2010.

[21] J. Bernholc, D. Brenner, M. Buongiorno Nardelli, V. Meunier, and C. Roland, "Mechanical and electrical properties of nanotubes," *Annu. Rev. Mater. Res.*, vol. 32, no. 1, pp. 347–375, 2002.

[22] P. Costa, J. Silva, A. Ansón-Casaos, M. T. Martinez, M. J. Abad, J. Viana, and S. Lanceros-Mendez, "Effect of carbon nanotube type and functionalization on the electrical, thermal, mechanical and electromechanical properties of carbon nanotube/styrene–butadiene–styrene composites for large strain sensor applications," *Compos. Part B Eng.*, vol. 61, pp. 136–146, 2014.

[23] A. A. Balandin, "Thermal properties of graphene and nanostructured carbon materials," *Nat. Mater.*, vol. 10, no. 8, pp. 569–581, 2011.

[24] R. Shah, T. Datashvili, T. Cai, J. Wahrmund, B. Menard, K. P. Menard, W. Brostow, and J. Perez, "Effects of functionalised reduced graphene oxide on frictional and wear properties of epoxy resin," *Mater. Res. Innov.*, vol. 19, no. 2, pp. 97–106, 2015.

[25] T. Jawhari, A. Roid, and J. Casado, "Raman spectroscopic characterization of some commercially available carbon black materials," *Carbon*, vol. 33, no. 11, pp. 1561–1565, 1995.

[26] F. Klauser, D. Steinmüller-Nethl, R. Kaindl, E. Bertel, and N. Memmel, "Raman Studies of Nano-and Ultra-nanocrystalline Diamond Films Grown by Hot-Filament CVD," *Chem. Vap. Depos.*, vol. 16, no. 4–6, pp. 127–135, 2010.

[27] Dongju Zhang and R. Q. Zhang, "Signature of nanodiamond in Raman spectra: a density functional theoretical Study," *J. Phys. Chem. B*, vol. 109, no. 18, pp. 9006–9013, 2005.

[28] Y. Bai, X. Zhao, T. Li, Z. Lv, S. Lv, H. Han, Y. Yin, and H. Wang, "First-principles investigation in the Raman and infrared spectra of sp 3 carbon allotropes," *Carbon*, vol. 78, pp. 70–78, 2014.

[29] E. J.-C. Amieva, R. Fuentes-Ramirez, A. L. Martinez-Hernandez, B. Millan-Chiu, L. M. Lopez-Marin, V. M. Castaño, and C. Velasco-Santos, "Graphene oxide and reduced graphene oxide modification with polypeptide chains from chicken feather keratin," *J. Alloys Compd.*, 2014.

[30] Y. Estévez-Martínez, C. Velasco-Santos, A.-L. Martínez-Hernández, G. Delgado, E. Cuevas-Yáñez, D. Alaníz-Lumbreras, S. Duron-Torres, and V. M. Castaño, "Grafting of

multiwalled carbon nanotubes with chicken feather keratin," *J. Nanomater.*, vol. 2013, p. 38, 2013.

[31] R. A. DiLeo, B. J. Landi, and R. P. Raffaelle, "Purity assessment of multiwalled carbon nanotubes by Raman spectroscopy," *J. Appl. Phys.*, vol. 101, no. 6, p. 064307, 2007.

[32] M. Begliarbekov, O. Sul, S. Kalliakos, E.-H. Yang, and S. Strauf, "Determination of edge purity in bilayer graphene using μ-Raman spectroscopy," *Appl. Phys. Lett.*, vol. 97, no. 3, p. 031908, 2010.

[33] W. Fortunato, A. J. Chiquito, J. C. Galzerani, and J. R. Moro, "Crystalline quality and phase purity of CVD diamond films studied by Raman spectroscopy," *J. Mater. Sci.*, vol. 42, no. 17, pp. 7331–7336, 2007.

[34] M. S. Dresselhaus, A. Jorio, A. G. Souza Filho, and R. Saito, "Defect characterization in graphene and carbon nanotubes using Raman spectroscopy," *Philos. Trans. R. Soc. Lond. Math. Phys. Eng. Sci.*, vol. 368, no. 1932, pp. 5355–5377, 2010.

[35] V. M. Irurzun, M. P. Ruiz, and D. E. Resasco, "Raman intensity measurements of single-walled carbon nanotube suspensions as a quantitative technique to assess purity," *Carbon*, vol. 48, no. 10, pp. 2873–2881, 2010.

[36] D. Nishide, Y. Miyata, K. Yanagi, T. Tanaka, and H. Kataura, "PERIPUTOS: Purity evaluated by Raman intensity of pristine and ultracentrifuged topping of single-wall carbon nanotubes," *Phys. Status Solidi B*, vol. 246, no. 11–12, pp. 2728–2731, 2009.

[37] A. C. Dillon, M. Yudasaka, and M. S. Dresselhaus, "Employing Raman spectroscopy to qualitatively evaluate the purity of carbon single-wall nanotube materials," *J. Nanosci. Nanotechnol.*, vol. 4, no. 7, pp. 691–703, 2004.

[38] Y. Miyata, K. Mizuno, and H. Kataura, "Purity and defect characterization of single-wall carbon nanotubes using Raman spectroscopy," *J. Nanomater.*, vol. 2011, p. 18, 2011.

[39] T. W. Zerda, W. Xu, A. Zerda, Y. Zhao, and R. B. Von Dreele, "High pressure Raman and neutron scattering study on structure of carbon black particles," *Carbon*, vol. 38, no. 3, pp. 355–361, 2000.

[40] E. Ebner, D. Burow, J. Panke, A. Börger, A. Feldhoff, P. Atanassova, J. Valenciano, M. Wark, and E. Rühl, "Carbon blacks for lead-acid batteries in micro-hybrid applications–Studied by transmission electron microscopy and Raman spectroscopy," *J. Power Sources*, vol. 222, pp. 554–560, 2013.

[41] O. A. Williams, *Nanodiamond*. The Royal Society of Chemistry, 2014.

[42] Z. Sun, Y. Sun, Q. Yang, X. Wang, and Z. Zheng, "IR spectral investigation of the pyrolysis of polymer precursor to diamond-like carbon," *Surf. Coat. Technol.*, vol. 79, no. 1, pp. 108–112, 1996.

[43] Y. Guo, Y. Guo, and C. Dong, "Ultrasensitive and label-free electrochemical DNA biosensor based on water-soluble electroactive dye azophloxine-functionalized graphene nanosheets," *Electrochimica Acta*, vol. 113, pp. 69–76, 2013.

[44] F. Lorestani, Z. Shahnavaz, P. Mn, Y. Alias, and N. S. Manan, "One-step hydrothermal green synthesis of silver nanoparticle-carbon nanotube reduced-graphene oxide composite and its application as hydrogen peroxide sensor," *Sens. Actuators B Chem.*, vol. 208, pp. 389–398, 2015.

[45] A. Benvidi, N. Rajabzadeh, M. Mazloum-Ardakani, and M. M. Heidari, "Comparison of impedimetric detection of DNA hybridization on chemically and electrochemically

functionalized multi-wall carbon nanotubes modified electrode," *Sens. Actuators B Chem.*, vol. 207, pp. 673–682, 2015.

[46] J. Mona, J.-S. Tu, T.-Y. Kang, C.-Y. Tsai, E. Perevedentseva, and C.-L. Cheng, "Surface modification of nanodiamond: photoluminescence and Raman studies," *Diam. Relat. Mater.*, vol. 24, pp. 134–138, 2012.

[47] M. Yu, Y. Huang, C. Li, Y. Zeng, W. Wang, Y. Li, P. Fang, X. Lu, and Y. Tong, "Building Three-Dimensional Graphene Frameworks for Energy Storage and Catalysis," *Adv. Funct. Mater.*, vol. 25, no. 2, pp. 324–330, 2015.

[48] M. Hernández-Ortiz, L. S. Acosta-Torres, G. Hernández-Padrón, A. I. Mendieta, R. Bernal, C. Cruz-Vázquez, and V. M. Castaño, "Biocompatibility of crystalline opal nanoparticles," *Biomed. Eng. Online*, vol. 11, no. 1, p. 78, 2012.

[49] Z. Y. Liu, J. L. Zhang, P. T. Yu, J. X. Zhang, R. Makharia, K. L. More, and E. A. Stach, "Transmission electron microscopy observation of corrosion behaviors of platinized carbon blacks under thermal and electrochemical conditions," *J. Electrochem. Soc.*, vol. 157, no. 6, pp. B906–B913, 2010.

[50] A. Lopez-Reyes, G. Orozco-Rivera, K. Acuna-Askar, J. F. Villarreal-Chiu, and J. M. Alfaro-Barbosa, "Characterization of atmospheric black carbon in particulate matter over the Monterrey metropolitan area, Mexico, using scanning electron microscopy," *Air Qual. Atmosphere Health*, pp. 1–7, 2015.

[51] Y. Estévez-Martínez, C. Velasco-Santos, A. L. Martínez-Hernández, G. Delgado, J. Arenas-Alatorre, S. Durón-Torres, D. Alaniz-Lumbreras, and V. M. Castaño,

"Characterization of nanostructures of oxidized multiwalled carbon nanotubes –G–keratin hybrids by transmission electron microscopy," *ScienceJet*, vol. 4, p. 108, 2015.



 

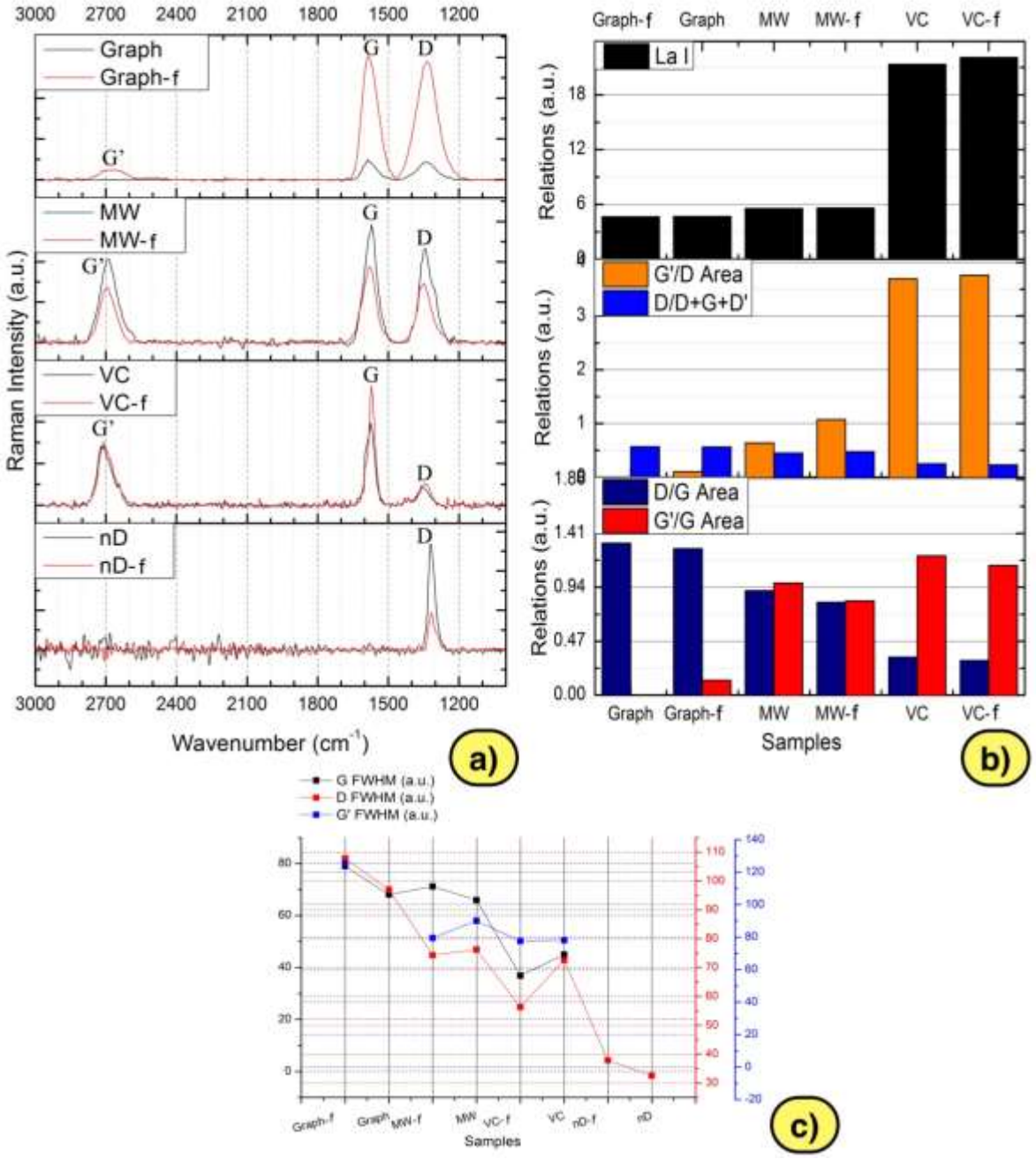


**Figure 1. a) Raman spectra for each carbon allotrope, b) Calculated areas and relationship among them, c) FWHM plotted.**

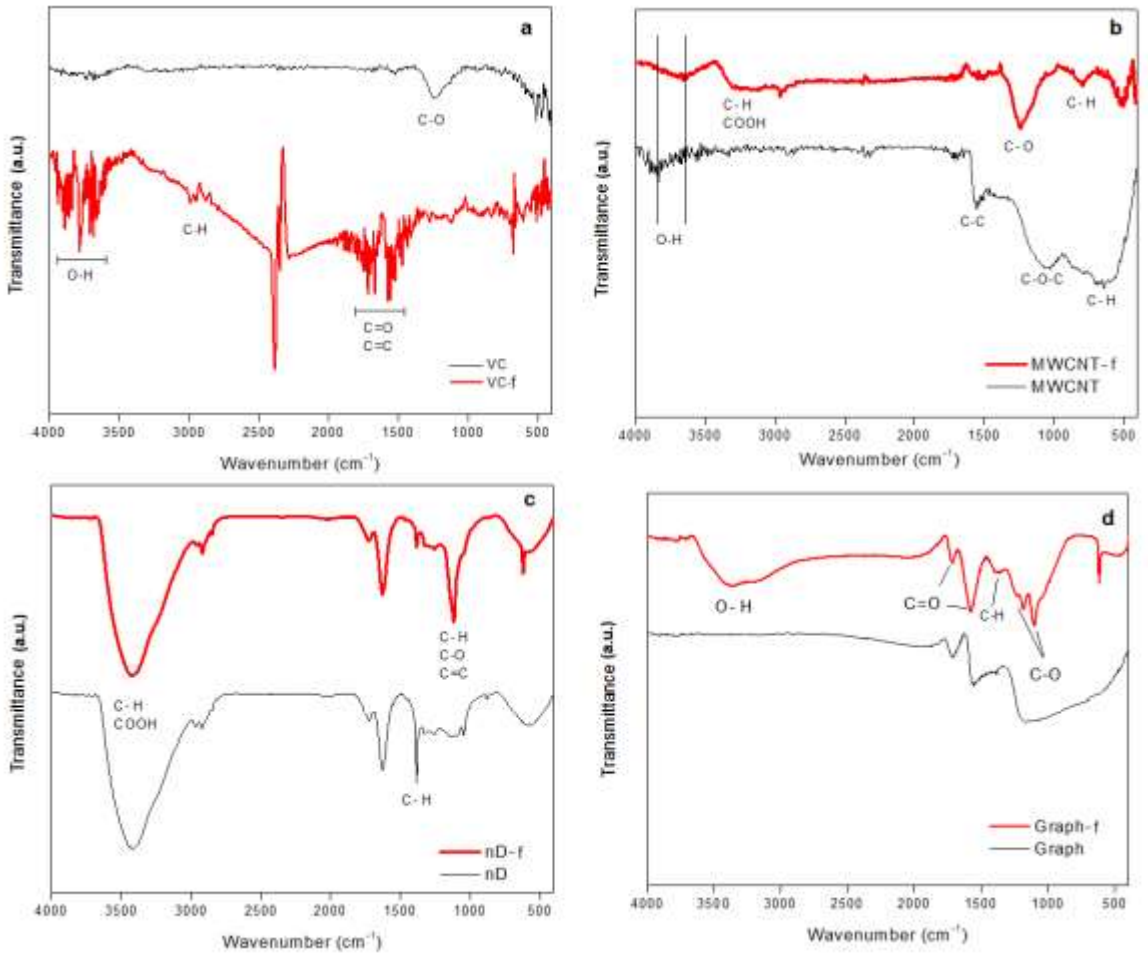


**Figure 2. IR spectra of functionalized and unfunctionalized carbons: (a) VC, (b) MWCNT, (c) nD, and (d) Graph**

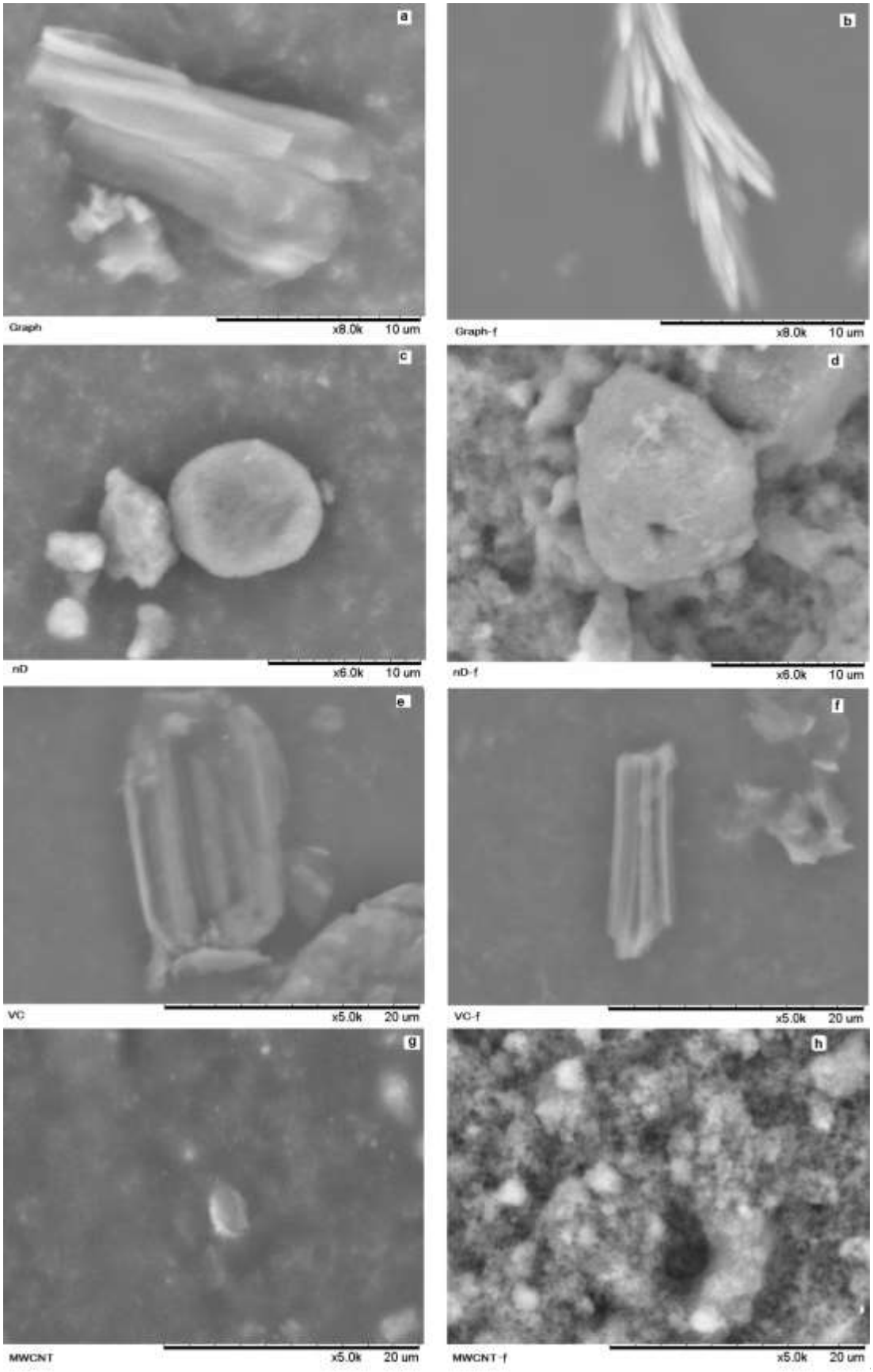

**Figure 3. SEM images of the carbon nanoallotropes (a and b) Graph, Graph-f; (c and d) nD, nD-f; (e and f) VC, VC-f; and (g and h) MW, MW-f, respectively.**



 

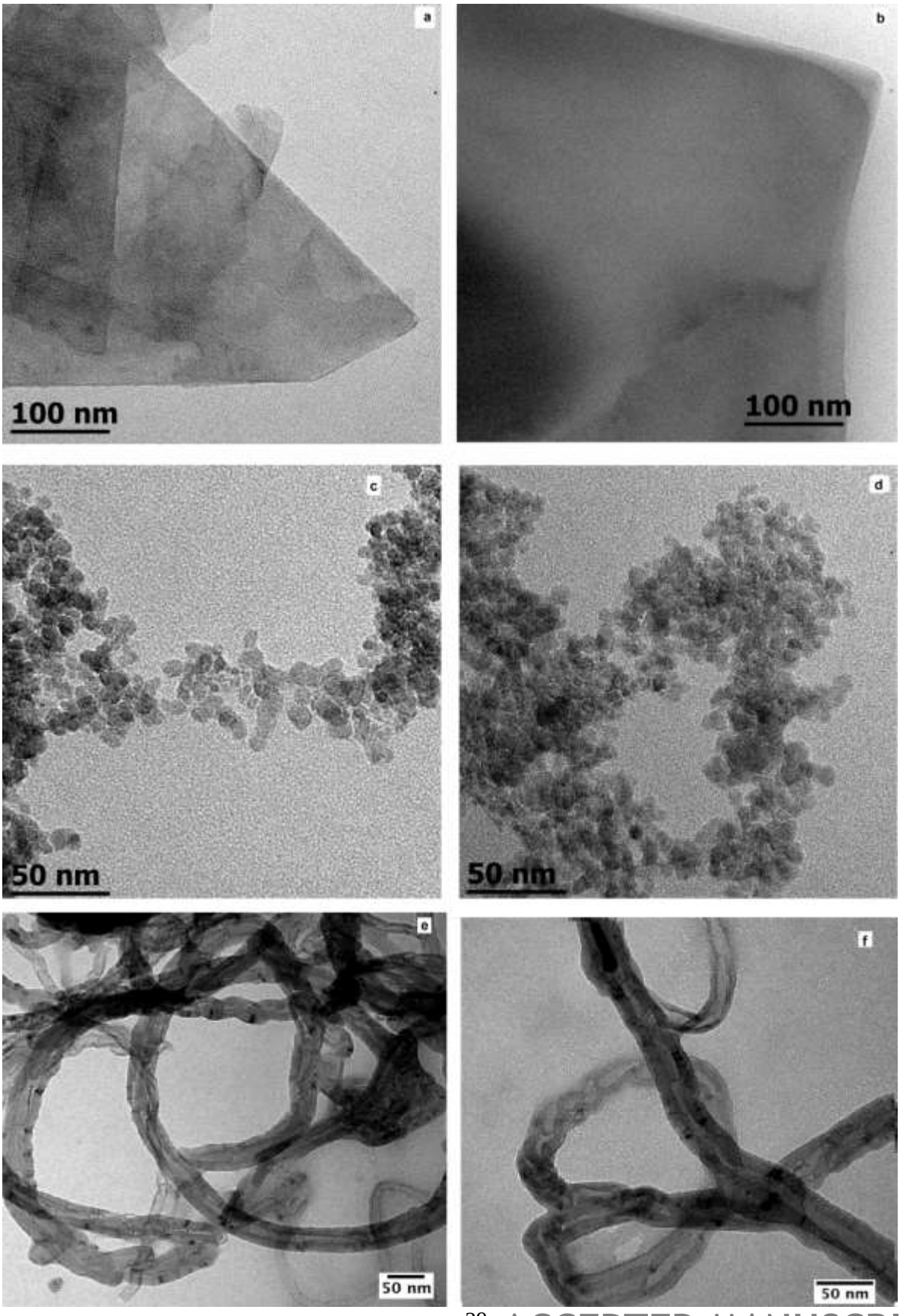




 

**Figure 4. TEM images of a) VC, b) VC-f, c) nD, d) nD-f, e) MW and f) MW-f.**



 